

Self-inductance of chiral conducting nanotubes

Yoshiyuki Miyamoto

Fundamental Research Laboratories, NEC Corporation, 34 Miyukigaoka, Tsukuba 305-8501, Japan

Angel Rubio

Departamento de Física Teórica, Universidad de Valladolid, E-47011 Valladolid, Spain

Steven G. Louie and Marvin L. Cohen

*Department of Physics, University of California at Berkeley, Berkeley, California 94720-7300
and Material Science Division, Lawrence Berkeley National Laboratory, Berkeley, California 94720*

(Received 11 June 1998)

Chiral conductivity in nanotubes has recently been predicted theoretically. The realization and application of chiral conducting nanotubes can be of great interest from both fundamental and technological viewpoints. These chiral currents, if they are realized, can be detected by measuring the self-inductance. We have treated Maxwell's equations for chiral conducting nanotubes (nanocoils) and find that the self-inductance and the resistivity of nanocoils should depend on the frequency of the alternating current even when the capacitance of the nanocoils is not taken into account. This is in contrast to elementary treatment of ordinary coils. This fact is useful to distinguish nanocoils by electrical measurements. [S0163-1829(99)00843-7]

I. INTRODUCTION

Carbon nanotubes can be viewed as cylindrical forms of rolled graphene sheets¹ and most of them have chiral atomic arrangements.² Theoretical studies³⁻⁵ predict that these carbon nanotubes are either metallic or semiconducting depending on their diameters and geometrical chiralities. These theoretical predictions triggered extensive research in the conducting properties of nanotubes. Experiment has shown that conductances of individual nanotubes can vary^{6,7} suggesting that tubule conductivities depend on their geometries.

New classes of nanotubes consisting of the graphiticlike compounds, BN, BC₃, and BC₂N have been investigated theoretically,⁸⁻¹⁰ and synthesis of BN (Refs. 11-13) and B_xC_yN_z (Refs. 14 and 15) nanotubes has been realized. The geometrical structures of some of these compound nanotubes are not settled as yet. In the case of BC₂N, nanotubes doped with carriers should have unique conducting properties, that is chiral conductance.¹⁶ This is because the anisotropic conductivity of the BC₂N sheets results in chiral trajectories for the current density in the nanotubes. On the other hand, pure carbon nanotubes are not expected to be significant chiral conductors even when they have structural chirality. The graphitic walls of pure carbon nanotubes have nearly isotropic in-plane conductivities, which inhibits chiral currents.¹⁶ Mechanical stretching has been proposed as a method for inducing chiral conductivity in these carbon nanotubes when doped.¹⁷ The essence of chiral conduction is symmetry breaking on tubule walls upon mechanical stretching. This induced current chirality is most likely for geometrically chiral nanotube having helical pitches close to those of arm-chair tubules. The arm-chair nanotubes appear to be one of the main constituents in the single-walled carbon ropes observed in Ref. 18. Recently, atomically resolved scanning tunneling microscope measurements revealed the existence

of chiral nanotubes, some of which differ slightly from the arm-chair shape.¹⁹ These nanotubes can be used to check the predicted chirality under stretching. Hereafter, nanotubes with chiral conductivities are called nanocoils.

A question can be raised as to how chiral currents in nanocoils would be measured experimentally. One possible approach is to observe the selfinductance of nanocoils. When alternating current (AC) flows in nanocoils, the circular component of the current generates an alternating magnetic field that induces an electric field along the tubule circumference.

Since the nanocoils have very small diameters, one can imagine that quantum behavior in electron transport (coherent electronic transport) occurs. However, the lengths of nanocoils would be in the order of microns, same as nanotubes. This order of the lengths is far beyond the typical coherent lengths of electrons at room temperature because of considerable electron-phonon scatterings and of impurity scatterings. The coherent transport should be realized in perfect nanotubes only under extremely low temperatures. Although the regime of the quantum transport is an interesting subject, hereafter, we rather focus our attention on ordinary conditions of semiclassical transport which will be mostly realized in typical experimental situations.

Here, we present a classical treatment of Maxwell's equations for nanocoils. In this simple treatment, we assume the classical electron transport instead of quantum-mechanical treatment of electron hoppings.²⁰ This assumption enables us to evaluate the current-induced magnetic field easily. The selfinductance of the nanocoil is found to be frequency dependent even when there is no capacitance in the nanocoil itself. This result is contrary to the case of ordinary coils. In the limit of low frequencies ($\omega \rightarrow 0$), the effective inductance of a nanocoil is found to be a function of ω^2 . The basic physics behind this phenomenon is that in a nanocoil the chiral angle of the current is ω dependent whereas in a classical coil this is fixed by the pitch of the winding of the wires

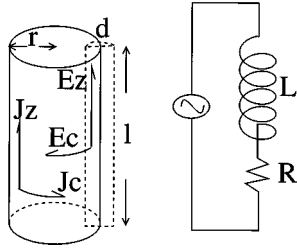


FIG. 1. Schematic diagram of a nanotube with chiral conductivity. The currents densities J_z and J_c are decomposed components of the chiral current density along the tubule axis z and circumference c , respectively. The electric fields E_z and E_c are also shown. The classical equivalent circuit of the entire system with nanocoil is also drawn for comparison.

in forming the coil. In the latter part of this paper, we show the derivation of this conclusion. In Sec. II, we formulate the classical Maxwell's equation for alternative currents in nanocoils. In Sec. III, we derive the ω^2 dependency of the self-inductance of the nanocoils and we summarize the present results in Sec. IV.

II. ELECTRODYNAMICAL TREATMENT OF NANOCOILS

We model the nanocoil as a continuous conducting cylinder with diameter r , length l , and an effective thickness d for current flow. For convenience, we use the two principal axes z and c in the directions of tubule axis and circumference, respectively. The chiral current density \mathbf{J} , which has the dimensions of (charge \times velocity)/(volume), can be decomposed into z and c components, J_z and J_c . An electric field \mathbf{E} can also be decomposed into z and c components, E_z and E_c , and we can relate \mathbf{J} to \mathbf{E} as following:

$$\begin{pmatrix} J_z \\ J_c \end{pmatrix} = \begin{pmatrix} \sigma_{zz} & \sigma_{zc} \\ \sigma_{cz} & \sigma_{cc} \end{pmatrix} \begin{pmatrix} E_z \\ E_c \end{pmatrix}. \quad (1)$$

Here, the tensor $\sigma_{\mu\nu}$ is the conductivity tensor for a nanotube, which can be obtained within the framework of Boltzmann's transport equation solved by using the relaxation time approximation^{16,17} or, in general, obtainable within the Kubo-Greenwood formalism depending on frequency. This local approximation is derived assuming that, at any time, the same force acts on each electron. This is not the case if the field varies in space. However, this approximation is valid whenever the wavelength of the field is long compared to the electronic mean-free path. When this is not the case, we need to resort to nonlocal theories of greater complexity. However, here we take E_z as the applied external electric field and assume that it is constant over the nanotube length and that the local approximation for the current is valid. The left panel in Fig. 1 shows the geometrical situation for the present assumptions.

Based on similar assumptions as before, we can express the electric displacement \mathbf{D} of the nanocoil by using the frequency-dependent dielectric function of the nanocoil $\epsilon_{\mu\nu}$ within a local approximation

$$\begin{pmatrix} D_z \\ D_c \end{pmatrix} = \begin{pmatrix} \epsilon_{zz} & \epsilon_{zc} \\ \epsilon_{cz} & \epsilon_{cc} \end{pmatrix} \begin{pmatrix} E_z \\ E_c \end{pmatrix}. \quad (2)$$

We here distinguish $\epsilon_{\mu\nu}$ from $\sigma_{\mu\nu}$: $\epsilon_{\mu\nu}$ comes from responses of localized electrons and ionic cores while $\sigma_{\mu\nu}$ comes from responses of delocalized electrons near the Fermi level.

The right panel of Fig. 1 depicts an equivalent circuit for our nanocoil system. We assume here a good Ohmic contact between the nanocoil and the electrodes. L and R in the right panel of Fig. 1 are inductance and resistance of a coil, respectively, in the classical sense. As far as we know, the assumed good Ohmic contact has not been achieved experimentally, instead there are effective capacitance due to ill contacts which give rise to single-electron transport through nanotubes.²¹ A discussion of current-induced magnetic field in quantum transport would require the framework of quantum electrodynamics, which is beyond the scope of the present paper. Recent experimental works have achieved the remarkable reduction of the contact resistance between nanotube and electrodes.²² Very recently, the achieved contact has been within a resistance of 23 Kilo-Ohm between the outer shell of the multiwall nanotube and metal electrodes.²³ Indeed, there is a lot of work nowadays to reduce even further the contact resistance. In fact, Tersoff²⁴ have proposed that the momentum conservation in the electron transport from the metal electrode to nanotube may play a key role in reducing the resistivity. Even if the interactions between the nanotube and electrode are only the Van der Waals type, there should be significant orbital interactions as an analogy of the graphite interlayer case.²⁵ So the difference between the original density of states at the Fermi levels in nanotubes and electrodes will be compensated reducing the contact resistance. We thus expect that in near future a lower resistivity will be achieved in which the capacitance arising from the electrical contact can be ignored.²⁶

In this paper, we shall restrict ourselves to normal classical conductivity of nanocoils and show that inductance of nanocoils differ from ordinary classical coils even in this regime. Note that a nanocoil itself has no capacitance in the present model since we assume continuous surface current density. From a practical viewpoint, we can consider an effective capacitance C coming from the electric wires connected to the nanocoil for the current measurement. However, there is a standard scheme in measuring L , eliminating the effect of C from the wires,²⁷ by constructing an entire circuit including a reference, to which a relative inductance \tilde{L} is measured. For the general purpose of nanocoil's inductance, it is, then, not necessary to include capacitance effect in our present discussion.

From now on we take each component of \mathbf{E} , \mathbf{D} , and \mathbf{J} in Eqs. (1) and (2) to be homogeneous on the tubule wall. If the tubule length l is extremely long compared to its radius r and thickness d for the current flow, we can assume that the magnetic field \mathbf{B} , generated by a chiral current, is constant inside the nanocoil. All quantum effects related to the quantization of the magnetic flux ($\phi = ch/2e = 2.07 \times 10^{-7}$ Gauss cm²) are neglected in the present description.

Now let us solve Maxwell's equations for the nanocoil (unless otherwise stated, we use CGS units),

$$\nabla \cdot \mathbf{D}(\mathbf{r}) = 4\pi\rho(\mathbf{r}), \quad (3)$$

$$\nabla \cdot \mathbf{B}(\mathbf{r}) = 0, \quad (4)$$

$$\nabla \times \mathbf{H}(\mathbf{r}) = \frac{4\pi}{c} \mathbf{J}(\mathbf{r}) + \frac{1}{c} \frac{\partial \mathbf{D}(\mathbf{r})}{\partial t}, \quad (5)$$

$$\nabla \times \mathbf{E}(\mathbf{r}) = -\frac{1}{c} \frac{\partial \mathbf{B}(\mathbf{r})}{\partial t}. \quad (6)$$

Since we consider no charge accumulation on the nanocoils, the right-hand side of Eq. (3) is zero. Using Stoke's theorem considering a cross section ld parallel to tubule axis, Eqs. (5) and (6) can be rewritten as

$$l \left(\frac{B_z}{\mu} - \frac{B_z^{ext}}{\mu^{ext}} \right) = \left(\frac{4\pi}{c} J_c + \frac{1}{c} \frac{\partial D_c}{\partial t} \right) ld, \quad (7)$$

$$l(E_z - E_z^{ext}) = -\frac{1}{c} \frac{\partial B_c}{\partial t} ld. \quad (8)$$

The magnetic field \mathbf{B} is also decomposed into z and c components. E_z , B_z , μ , and E_z^{ext} , B_z^{ext} , μ^{ext} are the electric field, magnetic field, and magnetic permeability inside and outside the nanocoil, respectively. Here the length l is extremely long compared to d , so we can ignore the magnetic field outside the nanocoil (B_z^{ext}), the contribution, which is restricted only at the edge of the nanocoil. Furthermore, the left-hand side of Eq. (8) is zero if we consider the continuity of the tangential electric field going from inside to outside the nanocoil. For the case of extremely thin tubules ($d \rightarrow 0$) the continuity of the time derivatives in Eqs. (7) and (8) makes their contribution zero when multiplied by d . In this limit, we have non zero contribution for Eqs. (7) and (8) only when we have the surface density current and the magnetic field, which is proportional to this surface density current (as is known for classical coils).

By considering Stoke's theorem with respect to another cross section πr^2 , perpendicular to the tubule axis, Eq. (6) can be rewritten as,

$$2\pi r E_c + \frac{\pi r^2}{c} \frac{\partial B_z}{\partial t} = 0. \quad (9)$$

Using Eqs. (7) to (9) and adopting the definitions of Eqs. (1) and (2), we finally obtain an equation of motion for the electric field components E_z and E_c as,

$$2E_c + \frac{\mu r d}{c} \left(\frac{4\pi}{c} \sigma_{cz} \frac{\partial E_z}{\partial t} + \frac{4\pi}{c} \sigma_{cc} \frac{\partial E_c}{\partial t} + \frac{\epsilon_{cz}}{c} \frac{\partial^2 E_z}{\partial t^2} + \frac{\epsilon_{cc}}{c} \frac{\partial^2 E_c}{\partial t^2} \right) = 0. \quad (10)$$

Here, we assume E_z is the applied external field $E_z \cos(\omega t)$, and then solve for the induced field E_c by assuming that $E_c = E'_c \cos(\omega t) + E''_c \sin(\omega t)$. By taking the $\cos(\omega t)$ and $\sin(\omega t)$ terms separately, and defining a material dependent constant $T = \mu r d / c^2$, we obtain

$$\begin{pmatrix} 2 - T\omega^2 \epsilon_{cc}(\omega) & 4\pi T\omega \sigma_{cc}(\omega) \\ -4\pi T\omega \sigma_{cc}(\omega) & 2 - T\omega^2 \epsilon_{cc}(\omega) \end{pmatrix} \begin{pmatrix} E'_c \\ E''_c \end{pmatrix} = \begin{pmatrix} T\omega^2 \epsilon_{cz}(\omega) E_z \\ 4\pi T\omega \sigma_{cz}(\omega) E_z \end{pmatrix}, \quad (11)$$

which can be solved taking into account the ω dependence of $\epsilon_{\mu\nu}$ and $\sigma_{\mu\nu}$. The final result for the induced circular electric field is

$$E'_c = T\omega \frac{\{2 - T\omega^2 \epsilon_{cc}(\omega)\} \omega \epsilon_{cz}(\omega) - (4\pi)^2 T\omega \sigma_{cc}(\omega) \sigma_{cz}(\omega)}{\{2 - T\omega^2 \epsilon_{cc}(\omega)\}^2 + \{4\pi T\omega \sigma_{cc}(\omega)\}^2} E_z, \quad (12)$$

$$E''_c = 4\pi T\omega \frac{T\omega^2 \sigma_{cc}(\omega) \epsilon_{cz}(\omega) + \{2 - T\omega^2 \epsilon_{cc}(\omega)\} \sigma_{cz}(\omega)}{\{2 - T\omega^2 \epsilon_{cc}(\omega)\}^2 + \{4\pi T\omega \sigma_{cc}(\omega)\}^2} E_z. \quad (13)$$

For the experimental determination of the selfinductance, we must measure J_z since the other component of the current J_c , along tubule circumference, is not extractable. Then expressing J_z as $J'_z \cos(\omega t) + J''_z \sin(\omega t)$, we finally obtain

$$J'_z = \sigma_{zz}(\omega) E_z + \sigma_{zc}(\omega) E'_c = \left[\sigma_{zz}(\omega) + \sigma_{zc}(\omega) T\omega^2 \frac{\{2 - T\omega^2 \epsilon_{cc}(\omega)\} \epsilon_{cz}(\omega) - (4\pi)^2 T\sigma_{cc}(\omega) \sigma_{cz}(\omega)}{\{2 - T\omega^2 \epsilon_{cc}(\omega)\}^2 + \{4\pi T\omega \sigma_{cc}(\omega)\}^2} \right] E_z, \quad (14)$$

$$J''_z = \sigma_{zc}(\omega) E''_c = 4\pi T\omega \sigma_{zc}(\omega) \frac{T\omega^2 \sigma_{cc}(\omega) \epsilon_{cz}(\omega) + \{2 - T\omega^2 \epsilon_{cc}(\omega)\} \sigma_{cz}(\omega)}{\{2 - T\omega^2 \epsilon_{cc}(\omega)\}^2 + \{4\pi T\omega \sigma_{cc}(\omega)\}^2} E_z. \quad (15)$$

For an applied voltage V_0 and nanocoil length l , E_z in the previous equations corresponds to V_0/l . We stress that this is an approximation that stems from our model description of the nanocoil current. Considering a practical experimental situation, the possible range of ω is limited to a low-frequency regime in which both $\sigma_{\mu\nu}$ and $\epsilon_{\mu\nu}$ are well approximated as their values at $\omega=0$. On the other hand, in the classical case of a resistance R and a inductance L in series (see the right panel in Fig. 1) the total current I is given as

$$I' = \frac{R}{R^2 + \left(\frac{L\omega}{c^2}\right)^2} V_0, \quad (16)$$

$$I'' = \frac{L\omega/c^2}{R^2 + \left(\frac{L\omega}{c^2}\right)^2} V_0, \quad (17)$$

here I' and I'' are the $\cos(\omega t)$ and $\sin(\omega t)$ components of I , respectively. Then, we can relate R and L with I' and I'' as,

$$R = \frac{I' V_0}{I'^2 + I''^2}, \quad (18)$$

$$L = \left(\frac{c^2}{\omega}\right) \frac{I'' V_0}{I'^2 + I''^2}. \quad (19)$$

Similarly, we can derive an effective inductance of the nanocoil (\tilde{L}) and a resistance (\tilde{R}) as follows,

$$\tilde{R} = \frac{J'_z V_0}{(J'^2_z + J''^2_z)(2\pi r d)}, \quad (20)$$

$$\tilde{L} = \left(\frac{c^2}{\omega}\right) \frac{J''_z V_0}{(J'^2_z + J''^2_z)(2\pi r d)}. \quad (21)$$

Here, the factor of $2\pi r d (= \int_{r-d/2}^{r+d/2} 2\pi r' dr')$ corresponds to the cross section for current density J_z according to the present geometrical assumption, see left panel of Fig. 1. By plugging Eqs. (14) and (15) into Eqs. (20) and (21), both \tilde{R} and \tilde{L} are found to be ω dependent even though all elements of $\sigma_{\mu\nu}$ and $\epsilon_{\mu\nu}$ are set to be constant. This fact is in a sharp contrast to the cases of classical coils. Furthermore, both \tilde{R} and \tilde{L} are found to be functions of ω^2 from the functional form of Eqs. (14) and (15) and those of Eqs. (20) and (21).

III. ω DEPENDENCE OF THE SELF-INDUCTANCE OF NANOCOILS

With use of above equations, we now focus on how \tilde{L} behaves at low- ω regime. First, let us define $\Theta \equiv \omega^2$ and introduce the following definitions

$$\alpha(\Theta) \equiv (2 - T\Theta \epsilon_{cc})^2 + (4\pi T\sigma_{cc})^2 \Theta, \quad (22)$$

$$\beta(\Theta) \equiv (2 - T\Theta \epsilon_{cc}) \epsilon_{cz} - (4\pi)^2 T\sigma_{cc} \sigma_{cz}, \quad (23)$$

$$\gamma(\Theta) \equiv T\sigma_{cc} \epsilon_{cz} \Theta + (2 - T\Theta \epsilon_{cc}) \sigma_{cz}, \quad (24)$$

$$f(\Theta) \equiv \{\sigma_{zz} \alpha(\Theta) + \sigma_{zc} T\Theta \beta(\Theta)\}^2 + \{4\pi T\sigma_{zc} \gamma(\Theta)\}^2 \Theta, \quad (25)$$

$$g(\Theta) \equiv \alpha(\Theta) \gamma(\Theta). \quad (26)$$

Combining Eqs. (14), (15), and (21) with above Eqs. (22)–(26), one can obtain

$$\tilde{L} = \frac{g(\Theta)}{f(\Theta)} \left(\frac{4\pi T\sigma_{zc} l c^2}{2\pi r d} \right). \quad (27)$$

In the low-frequency limit, the autoinductance \tilde{L} has a finite value of $2\pi c^2 T l \sigma_{zc} \sigma_{cz} / (2\pi r d \sigma_{zz}^2)$ because $J''_z(\omega)/\omega$ is nonzero when $\omega \rightarrow 0$. However, what matters for the impedance of the system is $\omega \tilde{L}$ and this is zero, in agreement with the fact that in static fields there are no contribution of inductive effects. By performing a Taylor expansion of \tilde{L} around $\Theta=0$ ($\omega=0$), we get the ω^2 dependence at low-frequency limit. Our current interest is in the sign of the first derivative of \tilde{L} with respect to Θ , which determines whether \tilde{L} increases or decreases with increasing frequency. The sign of the first derivative corresponds to that of the sign of the function S with

$$\begin{aligned} S &= \dot{g}(0)f(0) - \dot{f}(0)g(0) \\ &= -(\sigma_{zz})^2 \alpha(0)^2 \dot{\alpha}(0) \gamma(0) + (\sigma_{zz})^2 \alpha(0)^3 \dot{\gamma}(0) \\ &\quad - 2\sigma_{zz} \sigma_{zc} T \alpha(0)^2 \beta(0) \gamma(0) - (4\pi T \sigma_{zc})^2 \alpha(0) \gamma(0)^3, \end{aligned} \quad (28)$$

where dots mean the first derivative with respect to Θ . From the definitions (22) to (24), we know

$$\alpha(0) = 4, \quad (29)$$

$$\dot{\alpha}(0) = (4\pi T \sigma_{cc})^2 - 4T \epsilon_{cc}, \quad (30)$$

$$\beta(0) = 2\epsilon_{cz} - (4\pi)^2 T \sigma_{cc} \sigma_{cz}, \quad (31)$$

$$\gamma(0) = 2\sigma_{cz}, \quad (32)$$

$$\dot{\gamma}(0) = T(\sigma_{cc} \epsilon_{cz} - \sigma_{cz} \epsilon_{cc}), \quad (33)$$

and they can be used to rewrite Eq. (28) as

$$\begin{aligned} S &= -\pi^2 2(4)^4 T^2 \sigma_{cz} \{\sigma_{zz} \sigma_{cc} - (\sigma_{cz})^2\}^2 \\ &\quad + 4^3 T \sigma_{zz} [\sigma_{zz} \sigma_{cz} \epsilon_{cc} + \{\sigma_{zz} \sigma_{cc} - 2(\sigma_{cz})^2\} \epsilon_{cz}]. \end{aligned} \quad (34)$$

For simplicity, we now consider a thin nanocoil having only one energy band crossing its Fermi level. Applying the Boltzmann's transport equation within constant relaxation time approximation, the conductivity tensor $\sigma_{\mu\nu}$ is proportional to $v_\mu v_\nu$,^{16,17} where v_μ and v_ν are the averaged Fermi velocities of electrons. Thus we can equate $\sigma_{cc} \sigma_{zz} = (\sigma_{cz})^2$, and Eq. (34) can be rewritten as

$$S = 4^3 T \sigma_{zz} \sigma_{cz} (\sigma_{zz} \epsilon_{cc} - \sigma_{cz} \epsilon_{cz}). \quad (35)$$

Then the sign of S is found to be dependent on the parameters σ_{cz} , σ_{zz} , ϵ_{cc} , and ϵ_{cz} . So the sign of the first derivative of the inductance with respect to ω^2 is a material dependent quantity. If a nanocoil has very high conductivity along tubule circumference compared to those along tubule axis (resulting in a high chiral pitch of the AC current), $\sigma_{cz} \epsilon_{cz}$ can be bigger than $\sigma_{zz} \epsilon_{cc}$ and then Eq. (35) is negative indicating a decay of \tilde{L} with increasing ω . In this case, the decay can be simply understood as that the current becomes less chiral with higher frequency in order to reduce the energy loss in the direction of the tubule circumference. On the other hand, if the contributions from localized electrons and ionic cores (expressed as $\epsilon_{\mu\nu}$) are negligible compared to those from delocalized electrons near the Fermi level, Eq. (35) has a very small value. In this case, the self-inductance of a nanocoil is nearly frequency independent in the low-frequency regime. This whole phenomenon arises from the fact that for nanocoils the chiral angle of the current [as given by Eq. (1)] is frequency dependent since E_c is frequency dependent.

IV. SUMMARY

We have obtained an expression for the autoinductance L in terms of the microscopic quantities of the nanocoil (conductivity and ionic dielectric tensors) and derived the I-V relation for nanocoils. We conclude that the selfinductance and resistance of nanocoils should depend on the square of the frequency, which can be tested experimentally and will be used as fingerprints of nanocoils.

ACKNOWLEDGMENTS

We thank Paul Delaney for a careful reading of the manuscript. Two of the authors (Y.M. and S.G.L.), respectively, thank F. Nihey and A. Zettl for fruitful discussions and comments from the experimental viewpoint. A.R. acknowledges financial support from European Community TMR Contract Nos. ERBFMRX-CT96-0067 (DG12-MIHT), DGES PB95-0720-C02-01, and DGICYT PB95-0202. S.G.L. and M.L.C. acknowledge support by the National Science Foundation Grant No. DMR-9520554 and the Office of Energy Research, Office of Basic Energy Sciences, Materials Sciences Division of the U. S. Department of Energy under Contract No. DE-AC03-76SF00098. S.G.L. also acknowledges the support of the Miller Institute for Basic Research in Science.

¹S. Iijima, Nature (London) **354**, 56 (1991).

²S. Iijima and T. Ichihashi, Nature (London) **363**, 603 (1993).

³N. Hamada, S. Sawada, and A. Oshiyama, Phys. Rev. Lett. **68**, 1579 (1992).

⁴R. Saito, M. Fujita, G. Dresselhaus, and M. S. Dresselhaus, Appl. Phys. Lett. **60**, 2204 (1992).

⁵X. Blase, L. X. Benedict, E. L. Shirley, and S. G. Louie, Phys. Rev. Lett. **72**, 1878 (1994); V. H. Crespi, M. L. Cohen, and A. Rubio, *ibid.* **79**, 2093 (1997).

⁶H. Dai, E. W. Wong, and C. M. Lieber, Science **272**, 523 (1996).

⁷T. W. Ebbesen, H. J. Lezec, H. Hiura, J. W. Bennet, H. F. Ghaemi, and T. Thio, Nature (London) **382**, 54 (1996).

⁸A. Rubio, J. L. Corkill, and M. L. Cohen, Phys. Rev. B **49**, R5081 (1994).

⁹X. Blase, A. Rubio, S. G. Louie, and M. L. Cohen, Europhys. Lett. **28**, 335 (1994).

¹⁰Y. Miyamoto, A. Rubio, S. G. Louie, and M. L. Cohen, Phys. Rev. B **50**, 18 360 (1994); Y. Miyamoto, A. Rubio, M. L. Cohen, and S. G. Louie, *ibid.* **50**, R4976 (1994).

¹¹P. Gleize, M. C. Schouler, P. Gadelle, and M. Caillet, J. Mater. Sci. **29**, 1575 (1994).

¹²N. G. Chopra, R. J. Luyken, K. Cherrey, V. H. Crespi, M. L. Cohen, S. G. Louie, and A. Zettl, Science **269**, 966 (1995).

¹³A. Loiseau, F. Willaime, N. Demoncy, G. Hug, and H. Pascard, Phys. Rev. Lett. **76**, 4737 (1996).

¹⁴O. Stephan, P. M. Ajayan, C. Colliex, P. Redlich, J. M. Lambert, P. Bernier, and P. Lefin, Science **266**, 1683 (1994).

¹⁵Z. Weng-Sieh, K. Cherrey, N. G. Chopra, X. Blase, Y. Miyamoto, A. Rubio, M. L. Cohen, S. G. Louie, A. Zettl, and R. Gronsky, Phys. Rev. B **51**, R11 229 (1995).

¹⁶Y. Miyamoto, S. G. Louie, and M. L. Cohen, Phys. Rev. Lett. **76**,

2121 (1996).

¹⁷Y. Miyamoto, Phys. Rev. B **54**, R11 149 (1996).

¹⁸A. Thess *et al.*, Science **273**, 483 (1996). The fibrous carbon ropes consist of up to 100 single-walled monodisperse nanotubes [with few microns in length, diameter 13.8 Å and chirality (10,10)] packed in a perfect triangular lattice with 17 Å lattice constant.

¹⁹J. W. G. Wildöer, L. C. Venema, A. G. Rinder, R. Smalley, and C. Dekker, Nature (London) **391**, 59 (1998); T. W. Odom, J. L. Huang, P. Kim, and C. M. Lieber, *ibid.* **391**, 62 (1998).

²⁰G. Y. Stepanyan, S. A. Maksimenko, A. Lakhtakia, O. M. Yevtushenko, and A. V. Gusakov, Phys. Rev. B **57**, 9485 (1998).

²¹M. Bockrath *et al.*, Science **275**, 1922 (1997); S. J. Tans *et al.*, Nature (London) **386**, 474 (1997).

²²A. Bachtold, M. Henry, C. Terrier, C. Strunk, C. Schönenberger, J.-P. Salvetat, J.-M. Bonard, and L. Forró, Appl. Phys. Lett. **73**, 274 (1998); P. J. Pablo, E. Graugnard, B. Walsh, R. P. Andres, S. Datta, and R. Reifengerger, *ibid.* **74**, 323 (1999).

²³R. Martel, T. Schmidt, H. R. Shea, T. Hertel, and Ph. Avouris, Appl. Phys. Lett. **73**, 2447 (1998).

²⁴J. Tersoff, Appl. Phys. Lett. **74**, 2122 (1999).

²⁵J.-C. Charlier, J.-P. Michenaud, and X. Gonze, Phys. Rev. B **46**, 4531 (1992).

²⁶Including the capacitance in our present theoretical framework is possible. However, we have found that the resulting formula will be rather complicated and that it is hard to extract the physical interpretation of the nanocoil self-inductance, which depends on the AC frequency as will be shown in the main text.

²⁷See, for example, *Electromagnetic Fields, Energy, and Forces*, edited by R. M. Fano, L. J. Chu, and R. B. Adler (Wiley, New York, 1960).